Heliyon 10 (2024) e37355

Contents lists available at ScienceDirect

Heliyon

journal homepage: www.cell.com/heliyon

Research article

Novel autosomal recessive SINO syndrome-associated *KIDINS220* variants provide insight into the genotype-phenotype correlation

Wenke Yang [a,b,c], Shuyue Wang [a,d], Xiaodong Huo [a], Ke Yang [a], Zhenglong Guo [a,b], Yanjun Li [a], Xinying Ji [c,**], Bingtao Hao [a,b], Shixiu Liao [a,b,*]

[a] *Henan Provincial People's Hospital, People's Hospital of Henan University, People's Hospital of Zhengzhou University, Zhengzhou, China*
[b] *National Health Commission Key Laboratory of Birth Defects Prevention, Henan Provincial Key Laboratory of Genetic Diseases and Functional Genomics, Zhengzhou, China*
[c] *School of Basic Medical Sciences, Henan University, Kaifeng, China*
[d] *Central Hospital of Wuhan, Wuhan, China*

ARTICLE INFO

Keywords:
SINO syndrome
KIDINS220 gene
Etiological variant
Genotype
Phenotype

ABSTRACT

Background: *KIDINS220* encodes a transmembrane scaffold protein, kinase D-interacting substrate of 220 kDa, that regulates neurotrophin signaling. Variants in *KIDINS220* have been linked to spastic paraplegia, intellectual disability, nystagmus, and obesity (SINO) syndrome or prenatal fatal cerebral ventriculomegaly and arthrogryposis (VENARG). This study aimed to investigate the genotype-phenotype correlation of pathogenic *KIDINS220* variants.
Methods: We performed whole-exome sequencing on a patient with SINO syndrome and epilepsy. Identified pathogenic variants were confirmed using Sanger sequencing and evaluated with *in silico* tools. A comprehensive literature review was conducted to analyze the genetic and phenotypic data of both the newly diagnosed patient and previously reported cases with *KIDINS220* variants.
Results: We identified novel compound heterozygous variants in *KIDINS220*, c.1556C > T (p.Thr519Met) and c.2374C > T (p.Arg792*), in the patient. Our analysis revealed that biallelic loss-of-function variants in *KIDINS220* are associated with VENARG or autosomal recessive SINO (AR-SINO), whereas carboxy-terminal truncated variants that escape nonsense-mediated mRNA decay and lack amino acid residues 1507–1529 are linked to autosomal dominant SINO (AD-SINO). Patients with AR-SINO exhibit more severe clinical features compared to those with AD-SINO.
Conclusions: Our study expands the spectrum of *KIDINS220* variants associated with AR-SINO and provides a valuable genotype-phenotype correlation for pathogenic *KIDINS220* variants.

1. Introduction

The *KIDINS220* gene, located on chromosome 2p25.1, encodes a transmembrane scaffold protein that interacts with various growth

* Corresponding author. Henan Provincial People's Hospital, People's Hospital of Henan University, People's Hospital of Zhengzhou University, Zhengzhou, 450003, China.
** Corresponding author. School of Basic Medical Sciences, Henan University, Kaifeng, 475004, China.
E-mail addresses: 10190096@vip.henu.edu.cn (X. Ji), ychslshx@henu.edu.cn (S. Liao).

https://doi.org/10.1016/j.heliyon.2024.e37355
Received 21 March 2024; Received in revised form 30 August 2024; Accepted 2 September 2024
Available online 2 September 2024

factor receptors, including tropomyosin receptor kinases (Trks) [1–3], p75 neurotrophin receptors ($p75^{NTR}$) [2,3], vascular endothelial growth factor receptors [4], and glutamatergic and gamma-aminobutyric acidergic (GABAergic) receptors [5]. *KIDINS220* and its receptors form a complex that regulates the PI3K-AKT and Ras-MAPK-ERK signaling pathways [4,6,7], influencing neuronal development, survival, growth, migration, differentiation, excitability and GABAergic synapses plasticity [5].

Previous studies have shown that alternative splicing isoforms of *KIDINS220* are expressed in different tissues, with highly spatiotemporal-specific expression patterns during fetal development [8]. The full-length transcript NM_020738.4 of human *KIDINS220* encodes a 220 kDa protein (NP_065789.1) containing 1771 amino acids. The protein comprises an amino-terminal ankyrin repeat-containing (ANK) domain, a central KAP NTPase P-loop domain with four transmembrane helices and a Trks binding region, and carboxy-terminal protein-protein interaction domains such as the proline-rich (PR) domain, CRKL interaction motif, sterile alpha motif (SAM)-like domain, kinesin light chain (KLC)-interacting motif (KIM), $p75^{NTR}$-binding region, and PDZ-binding region [1–3]. The functional diversity of each isoform arises from differences in the domains and cellular or subcellular localization of the encoded proteins.

In 2016, Josifova et al. reported three unrelated patients with heterozygous *de novo* protein-truncating variants in the last two exons of the *KIDINS220* gene that could escape nonsense-mediated mRNA decay (NMD). These patients exhibited unique syndrome phenotypes, including spastic paraplegia, intellectual disability, nystagmus, and obesity, collectively defined as SINO syndrome (OMIM #617296) [9]. Subsequent studies identified additional pathogenic protein-truncating *KIDINS220* variants causing autosomal dominant SINO syndrome (AD-SINO) [10–14], Zhang et al. demonstrated the potential gain-of-function of such truncated variants [14]. In 2017, Mero et al. reported a homozygous *KIDINS220* frameshift variant (c.3394_3403del, p.Gln1132Serfs*30) in three fetuses of a consanguineous couple [15]. This frameshift mutation at codon 1132 forms a premature termination codon (PTC) at codon 1162, potentially eliciting NMD and decreasing absolute expression levels [16,17]. Furthermore, homozygous frameshift (c.208del, p.Asp70Ilefs*18) and in-frame deletion (c.2137_2145del, p.Gln713_Leu715del) variants in the ANK and Trks binding regions, respectively, have been implicated in autosomal recessive prenatal lethal cerebral ventriculomegaly and arthrogryposis (VENARG) (OMIM #619501) in consanguineous families. Heterozygous carriers of c.208del, c.2137_2145del or c.3394_3403del in these families were described as healthy individuals [18,19]. Recently, Brady et al. described a surviving individual with compound heterozygous variants c.1263_1264delAA (p.Gln421Hisfs*11) and c.3718-12A > G (IVS27-12A > G) presenting with prenatal onset of cerebral ventriculomegaly and limb contracture, but not lethal, and postnatal clinical features consistent with AD-SINO but more severe [20]. The heterogeneity of *KIDINS220*-related clinical features appears to be influenced by the location of the variants [14]. However, a comprehensive understanding of the genotype-phenotype correlation for pathogenic *KIDINS220* variants requires further investigation.

In this study, we report the second case of autosomal recessive SINO syndrome (AR-SINO) caused by novel compound heterozygous variants in the *KIDINS220*. The variants c.1556C > T (p.Thr519Met) and c.2374C > T (p.Arg792*) were identified through a trio-based whole-exome sequencing (WES) approach. We conducted a genotype-phenotype correlation analysis using clinical features and genetic data from 30 patients, combining our findings with previous studies and gene transcripts [9–15,18–20]. This study expands the etiological and phenotypic spectrum of the *KIDINS220* gene in AR-SINO and provides potential genotype-phenotype correlations for pathogenic *KIDINS220* variants, aiding genetic counseling and clinical management.

2. Materials and methods

2.1. Clinical investigations

The proband, a 5.5-year-old girl, presented with spastic paraplegia, intellectual disability, language impairment, a stiff facial expression with salivation, binocular nystagmus and esotropia, plump cheeks, and obesity (body weight: 22.7 kg [85th percentile, weight-for-age]; height: 111 cm [33rd percentile, height-for-age]). She also had a history of epilepsy, beginning at 10 days old and characterized by increasing tonic convulsions. A neurodevelopmental examination at 30 months of age, performed according to Gesell Development Schedules, showed scores of 47, 32, 40, 49, and 48 in the domains of adaptation, gross motor, fine motor, language, and social behavior, respectively. Electroencephalography showed spike and wave activity with superimposed fast activity preceding seizures. Cranial magnetic resonance imaging was normal. Combination treatment with sodium valproate, lamotrigine, and phenobarbitone was ineffective. The proband's parents were nonconsanguineous and reported no family history of congenital abnormalities. There were no significant perinatal complications. To identify potential pathogenic genetic factors, peripheral blood samples were collected from the family. Informed consent was obtained, and the study was approved by the Ethics Committee of Henan Provincial People's Hospital (approval number: 2019_134).

2.2. Karyotype and chromosomal microarray analyses, trio-WES and Sanger sequencing

Karyotype and chromosomal microarray analyses were performed as previously described [21,22]. For trio-WES, genomic DNA was extracted from peripheral blood samples using the TIANamp Blood DNA Kit (Tiangen, Beijing, China). Exome capture was conducted with the AIExomeV2Plus Kit (iGeneTech, Beijing, China) and sequenced using the Illumina NovaSeq6000 system (Illumina, San Diego, CA, United States). After removing adaptors, PCR duplicates, and low-quality reads, the filtered reads were aligned to the human reference genome (GRCh37/hg19) using Burrows-Wheeler Aligner software (v0.7.15) [23]. Genomic variants were called using the Genome Analysis Toolkit (v4.0.10.0) pipeline [24] and annotated with ANNOVAR software [25]. Variant frequencies were initially evaluated in the Single Nucleotide Polymorphism Database (dbSNP) and Genome Aggregation Database (gnomAD) to exclude

single nucleotide polymorphism with minor allele frequencies greater than 1 %. Variants were classified according to the American College of Medical Genetics and Genomics guidelines [26]. Previously reported variants and associated phenotypes were filtered against databases including OMIM [27], ClinVar [28] and HGMD [29]. The identified variants were further verified in available family members and 1000 unrelated Chinese control individuals using Sanger sequencing.

2.3. Bioinformatics analysis

The potential pathogenicity of variants was evaluated using *in silico* tools MutationTaster (https://www.mutationtaster.org/), SIFT (http://provean.jcvi.org/index.php), PolyPhen2 (http://genetics.bwh.harvard.edu/pph2/) and ANNOVAR (https://annovar.openbioinformatics.org/en/latest/). Protein sequence conservation across *Homo sapiens*, *Mus musculus*, *Rattus norvegicus* and other species was assessed through multiple sequence alignment with Clustal Omega (https://www.ebi.ac.uk/tools/msa/clustalo/). Protein domain functional descriptions were annotated by InterPro (https://www.ebi.ac.uk/interpro/), UniProt (https://www.uniprot.org/) and previous studies [8,11,14,19]. Tertiary structure prediction was obtained from the AlphaFold protein structure database (https://alphafold.ebi.ac.uk/) and visualized with PyMOL (https://www.pymol.org/pymol.html). Isoform sequences for alignment analysis were retrieved from NCBI (https://www.ncbi.nlm.nih.gov/gene/) and Ensembl (http://asia.ensembl.org/index.html) databases.

2.4. Literature review

We conducted a comprehensive literature search in PubMed (https://pubmed.ncbi.nlm.nih.gov, accessed date: May 26, 2024) using keywords related to pathogenic *KIDINS220* variants and their associated clinical features. Studies involving copy number variations, other genetic variations, or lacking clinical details were excluded. We integrated clinical data and genetic information from retrieved publications with known transcript isoforms and protein domains to assess genotype-phenotype correlations.

3. Results

3.1. Genetic investigation revealed compound heterozygous mutations in the KIDINS220 gene in the patient

Karyotype and chromosomal microarray analyses revealed no chromosomal abnormalities in the family. Trio-WES identified compound heterozygous variants c.1556C > T (Chr2[GRCh37]:g.8930075, NP_065789.1:p.Thr519Met) and c.2374C > T (Chr2[GRCh37]:g.8919266, NP_065789.1:p.Arg792*) of *KIDINS220* (NM_020738.4) in the patient. Sanger sequencing confirmed that the proband's mother is a heterozygous carrier of the c.1556C > T variant, and her father is a heterozygous carrier of the c.2374C > T variant (Fig. 1A–C). Additionally, Sanger sequencing identified allele frequencies of 0.001 and 0 for c.1556C > T (p.Thr519Met) and c.2374C > T (p.Arg792*) in 1000 healthy, unrelated Chinese individuals, respectively. The c.1556C > T (p.Thr519Met) variant was predicted as deleterious by SIFT4G (score = 0.002), Polyphen2_HDIV (score = 1), MutationTaster (score = 1), CADD (score = 24.2) and, REVEL (score = 0.276). The CADD score indicated the c.2374C > T (p.Arg792*) was a potentially pathogenic variant (CADD score 38). According to ACMG guidelines, the c.1556C > T (p.Thr519Met) variant was classified as likely pathogenic (PM1), and c.2374C > T (p.Arg792*) was classified as pathogenic (PVS1 + PM2). No other known pathogenic or potentially pathogenic variations related to the proband's phenotype were found. Alignment showed high conservation of the mutated amino acid residues (Fig. 1D).

Both parents are asymptomatic carriers, suggesting a single copy wild-type *KIDINS220* is sufficient for a healthy phenotype. The potential loss-of-function of both variants suggested their pathogenicity. DeepTMHMM (https://dtu.biolib.com/DeepTMHMM) and Arpeggio (https://biosig.lab.uq.edu.au/arpeggioweb/) predicted the effect of p.Thr519Met on the first transmembrane helical segment and the hydrogen bonding interactions with amino acid residues. The results showed that the distribution of transmembrane region changed, and the hydrogen bonding interaction and bonding distance decreased (Fig. 1E). For c.2374C > T (p.Arg792 *), the PTC formed at codon 792 is located in the protein-coding region governed by NMD rules [16], which may elicit NMD and result in complete loss-of-function.

3.2. Heterogeneity of disease genetic patterns and phenotypes caused by pathogenic variants in KIDINS220

A comprehensive literature review identified 15 different *KIDINS220* genetic variants in this study (Fig. 2A) [9–15,18–20]. Frameshift variants (6/15, 40 %) and nonsense mutations (6/15, 40 %) are the most prevalent, followed by in-frame deletion (1/15, 6.7 %), splicing site variant (1/15, 6.7 %), and missense variant (1/15, 6.7 %). In 12 cases with biallelic pathogenic variants and phenotypic data, c.208del (p.Asp70Ilefs*18), c.2137_2145del (p.Gln713_Leu715del) or c.3394_3403del (p.Gln1132Serfs*30) is homozygous in 10 individuals (83.3 %) from three unrelated consanguineous families with VENARG, while two (16.7 %) compound heterozygous individuals exhibit AR-SINO [20]. Heterozygous carriers of these biallelic pathogenic variants were reported with healthy phenotypes [15,18–20]. Among the 18 cases carrying heterozygous truncated variants, 13 individuals with c.3934G > T (p.Glu1312*), c.4050G > A (p.Trp1350*), c.4096C > T (p.Gln1366*), c.4389_c.4390delAG (p.Ser1463Serfs*15), c.4520dup (p.Leu1507Phefs*4), c.3838delG (p.Glu1280Lysfs*54), or c.4177C > T (p.Gln1393*) exhibit typical AD-SINO, while five individuals carrying c.4448C > G (p.Ser1483*) are from a family with only sporadic paraplegia [11]. Overall, the clinical features of AR-SINO are more severe than those of AD-SINO, and the prenatal lethal VENARG caused by homozygous variation is the most severe. The clinical heterogeneity may be influenced by genetic patterns, the expression patterns of the *KIDINS220* isoforms, and the location of variations (Fig. 2A).

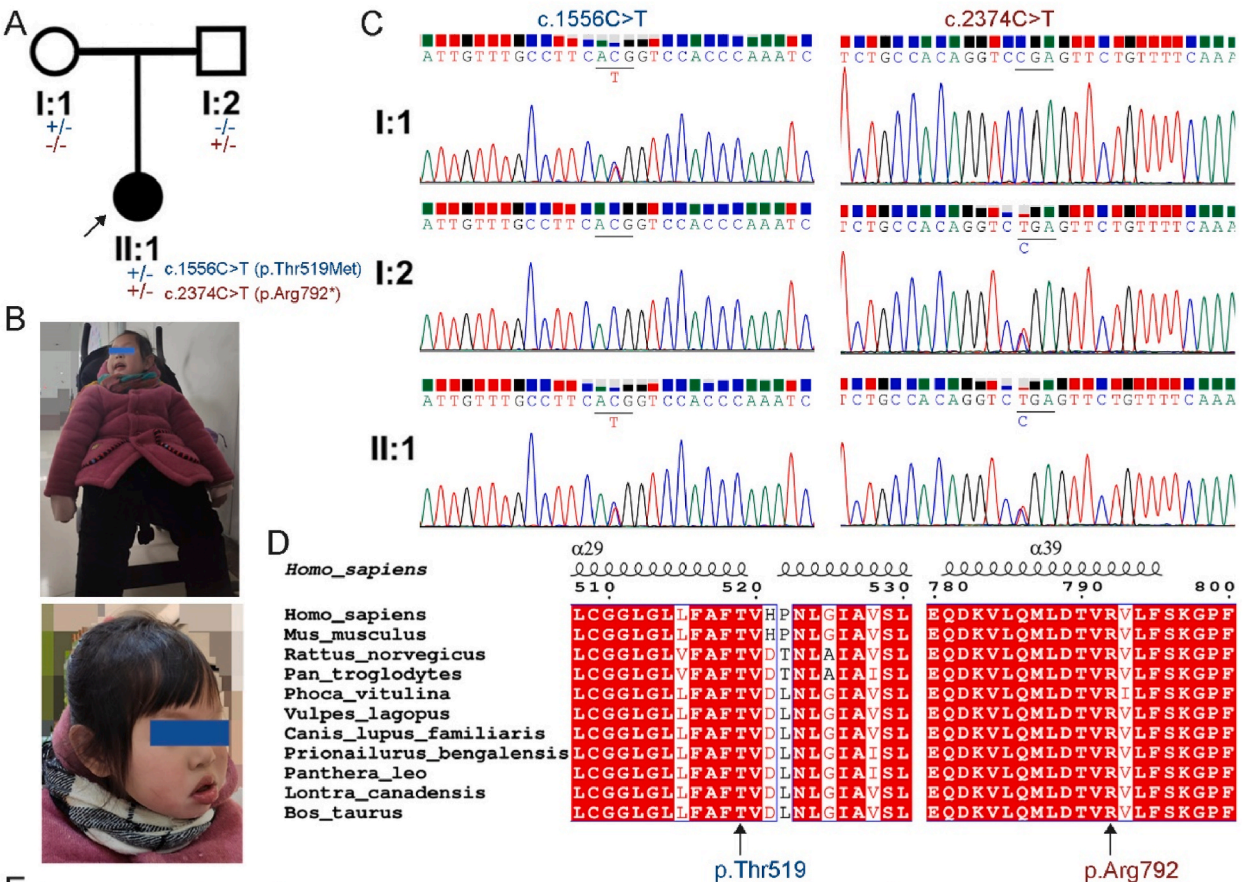

E

DeepTMHMM (KIDINS220_ wild type)	
distribution	range
inside	1-499
TMhelix	500-518
outside	519-524
TMhelix	525-545
inside	546-659
TMhelix	660-680
outside	681-690
TMhelix	691-706
inside	707-1771

DeepTMHMM (KIDINS220_ p.Thr519Met)	
distribution	range
inside	1-499
TMhelix	500-519
outside	520-524
TMhelix	525-545
inside	546-659
TMhelix	660-680
outside	681-690
TMhelix	691-706
inside	707-1771

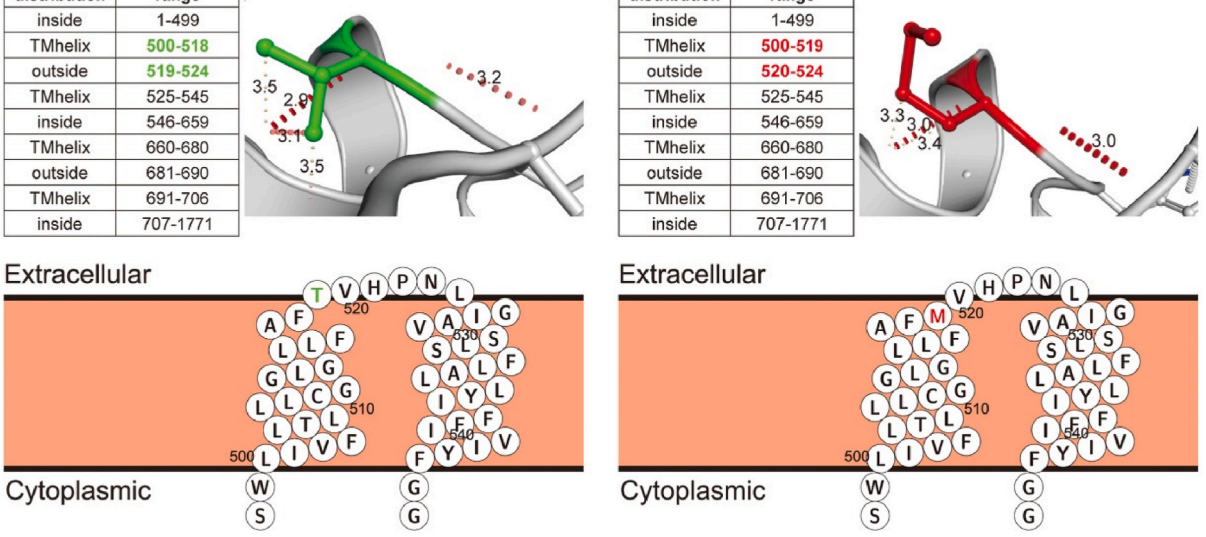

(caption on next page)

Fig. 1. Genetic analysis of *KIDINS220* gene in an affected family. (A) Pedigree of the investigated family showing an unaffected mother (I:1), an unaffected father (I:2), and an affected child (II:1). (B) The proband (II:1) exhibited clinical features such as bilateral lower limb spasticity and weakness, increased muscle tone, inability to stand or walk, intellectual disability and language impairment, stiff facial expression with salivation, binocular esotropia, and plump cheeks. (C) Sanger sequencing confirmed the presence of compound heterozygous variants c.1556C > T (p.Thr519Met) and c.2374C > T (p.Arg792*) in the proband (II:1). The unaffected mother (I:1) was heterozygous for the c.1556C > T variant (p.Thr519Met), and the unaffected father (I:2) was heterozygous for the c.2374C > T variant (p.Arg792*). (D) The *KIDINS220* p.Thr519 and p.Arg792 variants are conserved across various species. (E) Predicted impacts of p.Thr519Met on the sequence of the first transmembrane helical segment and the hydrogen bonding interactions with amino acid residues. Wild type is shown on the left and p.Thr519Met on the right.

3.3. Elucidating the potential genotype-phenotype correlation based on alternative RNA transcript isoforms and protein domains

Previous analyses of *KIDINS220* transcript isoforms have revealed expression patterns that are specific to cell subsets, spatio-temporal, and highly conserved among adult humans, rats, and mice [8]. Schmieg et al. reported that the m6 and m4 isoforms are primarily expressed in the brains of embryonic, postnatal and adult mice, while the alternative terminal exon C2 is scarcely expressed in the embryonic brain [8]. The m6 isoform, which skips exons 25–28, and the m4 isoform, which skips exons 24–28, provide valuable insights for inferring human embryonic brain isoforms. Sequence alignment showed that mouse exons 27–28 are absent in human sequences. The predominant alternative splicing isoforms in mouse embryonic brain tissue correspond to the skipping of exons 25 and 26 in the full-length transcript NM_020738.4 (Fig. 2B–Supplementary Table S1). Further multiple sequence alignment results indicated that 10 out of the 20 known isoform sequences encoding proteins, as provided by NCBI or Ensembl databases, were included as candidates for subsequent analysis due to the absence of exons 25, 26, and C2 Fig. 2C–Supplementary Table S2).

The c.208del (p.Asp70Ilefs*18) and c.3394_3403del (p.Gln1132Serfs*30) variants in the full-length transcript NM_020738.4 (NP_065789.1) have been reported as pathogenic for VENARG [15,18]. However, the corresponding p.Asp70 and p.Gln1132 sites are absent in transcripts ENST00000687912.1 (UniProt ID: A0A8I5KX08) and NM_001348745.2 (NP_001335674.1, UniProt ID: Q9ULH0-3), respectively, indicating that these transcripts are not functional isoforms causing VENARG (Fig. 2D). According to Josifova et al. [9], AD-SINO patients carrying the c.4050G > A (p.Trp1350*), c.4096C > T (p.Gln1366*) or c.4520dup (p.Leu1507Phefs*4) variants exhibit prenatal characteristics of lateral ventricular dilation and talipes equinovarus. This is consistent with Brady et al.'s report on prenatal characteristics of an AR-SINO patient carrying compound heterozygous variants c.1263_1264delAA (p.Gln421Hisfs*11) and c.3718-12A > G (IVS27-12A > G) [20]. Three transcripts, NM_001348734.2 (NP_001335663.1), NM_001344735.2 (NP_0001335664.1), and NM_001348736.2 (NP_001235665.1, UniProt ID: Q9ULH0-2), were identified as potential functional transcripts based on their inclusion of pathogenic variants associated with prenatal developmental abnormalities (Fig. 2C–D). Compared to NM_020738.4 (NP_065789.1), all three isoforms lack residues 1139–1195 encoded by exons 25–26, and none of the reported pathogenic variants are located within this region (Fig. 2A). Detailed sequence alignment results are presented in Supplementary Fig. S1. All three isoforms include the known *KIDINS220* (NP_065789.1) protein domains, the annotated functional domains and predicted tertiary structure are presented in Fig. 2D.

For the variants identified from VENARG and AR-SINO patients, the PTCs formed by the frameshift variants c.208del (p.Asp70Ilefs*18), c.3394_3403del (p.Gln1132Serfs*30), c.1263_1264delAA (p.Gln421Hisfs*11), and nonsense mutation c.2374C > T (p.Arg792*) are located in the protein-coding region governed by NMD rules, classifying these variants as NMD-elicit (Fig. 2A). Notably, c.208del (p.Asp70Ilefs*18) corresponds to c.82del (p.Asp28Ilefs*18) in the NM_001348736.2 (NP_001335665.1, UniProt ID: Q9ULH0-2) isoform, which is less than 150 nucleotides from the translation start site and could be classified as NMD-escape, forming polypeptides. In both cases, c.208del leads to a complete loss-of-function. The VENARG pathogenic in-frame deletion c.2137_2145del (p.Gln713_Leu715del) highlights the importance of the Trks interaction fragment in the KAP domain for normal embryonic development and results in a complete loss-of-function (Fig. 2A). The AR-SINO pathogenic splice site variant c.3718-12A > G (IVS27-12A > G) was predicted to format an abnormal splice acceptor site at 12 nucleotides upstream of the intron 27 consensus AG splice acceptor site, with an Acceptor Gain score 0.75 (SpliceAI). This disrupts the reading frame, resulting in a PTC of p.Ala1240Phefs*7 in the sequence encoding the SAM domain, and was classified as NMD-elicit (Fig. 2A). However, the consensus AG splice acceptor loss is not complete (SpliceAI score 0.78), which may preserve some normal transcripts. Therefore, c.3718-12A > G (IVS27-12A > G) is a partial loss-of-function allele. Consequently, the clinical phenotype of the case reported by Brady et al. is AR-SINO, not VENARG. Similarly, the AR-SINO case in this study suggests that the missense variant c.1556C > T (p.Thr519Met), predicted to affect amino acid distribution in the first transmembrane helical segment, is also a partial loss-of-function allele. It is also noteworthy that the parents of these VENARG and AR-SINO patients are heterozygous carriers without the VENARG or SINO phenotype, indicating that a monoallelic loss-of-function variant in the sequence encoding ANK, KAP, PR, or SAM domain, especially NMD-elicit variants, is tolerable for normal development. Biallelic loss-of-function variants in *KIDINS220* cause VENARG and AR-SINO, with the former resulting from two copies of complete loss-of-function and the latter from one copy of complete loss-of-function and one copy of partial loss-of-function.

AD-SINO patients harbor heterozygous pathogenic truncated variants, including c.3838delG (p.Glu1280Lysfs*54), c.3934G > T (p.Glu1312*), c.4050G > A (p.Trp1350*), c.4096C > T (p.Gln1366*), c.4177C > T (p.Q1393*), c.4389_c.4390delAG (p.Ser1463Serfs*15), c.4448C > G (p. Ser1483*) or c.4520dup (p.Leu1507Phefs*4). Located outside the NMD-governed region, these variants were classified as NMD-escape. However, Josifova et al. reported three *KIDINS220* heterozygous truncating variants p.Glu1530*, p.Arg1736*, and p.Ser1740*, in five healthy individuals [9]. These truncated proteins lack the carboxy-terminal $p75^{NTR}$ and PDZ-binding regions but retain the KIM region (Fig. 2A). Additionally, Zhang et al. reported a weak affinity between the gain-of-function truncated protein produced by variant c.4177C > T (p.Q1393*) and calpain-2 [14]. This evidence suggests that amino acid residues 1507–1529, following the KIM region, likely play a crucial role in the gain-of-function of truncated *KIDINS220* protein by

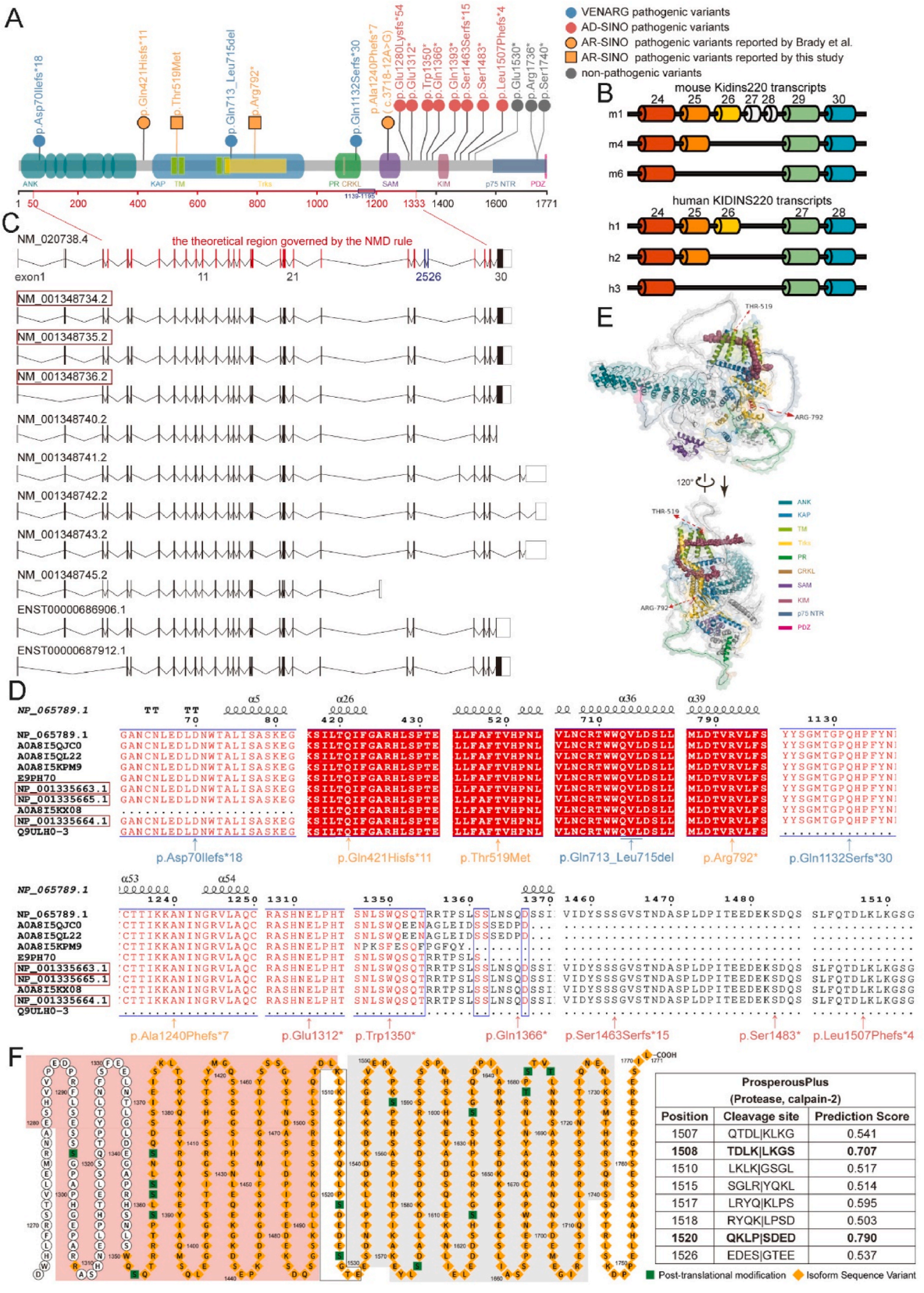

(caption on next page)

Fig. 2. KIDINS220 domain structure, identified variants distribution, and amino acid sequence alignment across different isoforms. (A) Domain organization of *KIDINS220* protein (NP_065789.1): ANK, Ankyrin repeat-containing domain (4-396aa); KAP, KAP NTPase P-loop domain (440-953aa); TM, transmembrane domains (500-520aa, 525-545aa, 660-680aa, 686-706aa); Trks, Trks binding region (693-891aa); PR, proline-rich stretch (1057-1151aa); CRKL, CRKL-interacting motif (1089-1092aa); SAM, sterile alpha motif-like domain (1207-1283aa); KIM, kinase light chain (KLC)-interacting motif (1406-1445aa); $p75^{NTR}$, $p75^{NTR}$ binding region (1591-1771aa); PDZ, PDZ binding region (1766-1771aa). (B) The *KIDINS220/Kidins220* transcripts described by Schmieg et al. [8]. (C) Ten known isoforms lack exons 25 and 26 of the full-length transcript NM_020738.4 and lack an alternative terminal exon C2 sequence. (D) Distribution of pathogenic variants across the *KIDINS220* protein isoforms. (E) Predicted tertiary structures of the *KIDINS220* protein with functional domains highlighted in distinct colors. (F) Predicted recognition sites of calpain-2 within the *KIDINS220* protein (1507–1529 aa) identified using the ProsperousPlus online server (http://prosperousplus.unimelb-biotools.cloud.edu.au/index.php). The distribution of AD-SINO pathogenic truncated variants (1280-1507aa, red-shaded area) and non-pathogenic truncated variants (1530-1740aa, gray-shaded area) suggests that the amino acid residues between the two regions may be crucial for determining variant pathogenicity (left). The predicted scores for amino acid residues K1508 and P1520 are 0.707 and 0.790, respectively (right).

affecting its affinity with calpain-2 (Fig. 2E). We further predicted calpain-2 recognition sites within these residues using the ProsperousPlus online server (http://prosperousplus.unimelb-biotools.cloud.edu.au/index.php). The prediction identified two potential high-scoring calpain-2 cleavage sites at residues K1508 (TDLK|LKGS) and P1520 (QKLP|SDED) (Fig. 2E). We propose that calpain-2 regulates protein degradation by recognizing these two key sites. The absence of these recognition sites is likely crucial for the functional gain observed in AD-SINO pathogenic truncated proteins. Therefore, the heterozygous gain-of-function variants involving the deletion of amino acid residues 1507–1529, especially K1508 and P1520, underlies AD-SINO.

4. Discussion

KIDINS220 plays a crucial role in neuronal plasticity, survival, growth, migration, and differentiation processes mediated by neurotrophins [6]. Neurotrophins induce alternative splice isoform expression in nerve cell clusters during embryonic development, reflecting the diverse neurotrophin-mediated signaling pathway requirements of each cell cluster under varying spatiotemporal conditions [8]. Studies on mice and human cells have demonstrated that *Kidins220* knockout or inadequate expression disrupts neurotrophin, vascular endothelial growth factor receptor, and kinesin-1-mediated signaling pathways during early fetal mouse development [4,7,30–32]. This disruption results in extensive neuronal cell death [4], lateral ventricular dilation [32], and severe cardiovascular system abnormalities [4]. Moreover, truncated *KIDINS220* protein produced by variant c.3934G > T (p.Glu1312*) is unable to maintain the phosphorylation of extracellular signal-regulated kinase, leading to uncontrolled differentiation and maturation of adipocytes [12]. These findings suggest that *KIDINS220* dysfunction is likely implicated in the pathophysiology of SINO syndrome or prenatal lethal VENARG by disrupting a series of signaling pathways.

The clinical phenotypes of VENARG include severe cerebral ventriculomegaly, limb contractures, cerebellar vermis hypoplasia, congenital heart disease, and hydrops fetalis in fetuses. AD-SINO syndrome, caused by heterozygous truncated variants, is characterized by spastic paraplegia, global developmental delay, intellectual disability, language impairment, decreased visual acuity, nystagmus, obesity, and plump cheeks [9–11]. Brain imaging reveals delayed myelination, lateral ventricular dilation, cerebral atrophy, and dysplasia of the corpus callosum. This study identified the novel compound heterozygous variants c.1556C > T (p.Thr519Met) and c.2374C > T (p.Arg792*) in a Chinese family. In addition to the typical phenotype described in previous literature, the patient in this study also presents with drug-refractory epilepsy, a previously unreported manifestation associated with *KIDINS220* gene mutation. Previous studies have shown no significant difference in the expression levels of *Kidins220* between excitatory glutamatergic neurons and inhibitory gamma-aminobutyric acidergic (GABAergic) neurons [5,33]. The constitutive absence of *Kidins220* does not affect basal synaptic transmission in either excitatory or inhibitory synapses [5]. However, under low-frequency pulse stimulation, significantly impaired inhibitory short-term synaptic plasticity [5], increased GABAergic neuronal excitability [33], and significantly reduced hippocampal network spiking activity [33] were observed. The potential pathophysiology of the proband presenting with epilepsy may involve functional loss of *KIDINS220* compound heterozygous variants leading to GABAergic dysfunctions, disrupting the balance of excitatory and inhibitory transmission in a neuronal network. The present case also supports the observation by Brady et al. that the AR-SINO disease phenotype is more severe than AD-SINO [20]. However, due to the lack of previous clinical records, we are unable to provide prenatal developmental data for this case.

Patients with different *KIDINS220* variants exhibit heterogeneous clinical phenotypes and genetic characteristics. This heterogeneity arises not only from genotype differences but also from the expression levels of various transcript isoforms in cell clusters [8], as well as the potential effects of variations on these isoforms. Based on the conserved expression patterns of splicing isoforms and their inclusion of pathogenic variants, three transcript isoforms, NM_001348734.2 (NP_001335663.1), NM_001348735.2 (NP_001335664.1), and NM_001348736.2 (NP_001335665.1, UniProt ID: Q9ULH0-2), were identified and considered as potential contributors to the prenatal phenotype of VENARG, AR-SINO, and AD-SINO patients.

We summarized the identified pathogenic variants of *KIDINS220*, including 6 frameshift mutations (c.208del (p.Asp70Ilefs*18), c.1263_1264delAA (p.Gln421Hisfs*11), c.3394_3403del (p.Gln1132Serfs*30), c.4389_c.4390delAG (p.Ser1463Serfs*15), c.4520dup (p.Leu1507Phefs*4), c.3838delG (p.Glu1280Lysfs*54)), 6 nonsense mutations (c.3934G > T (p.Glu1312*), c.4050G > A (p.Trp1350*), c.4096C > T (p.Gln1366*), c.4177C > T (p.Gln1393*), c.4448C > G (p.Ser1483*), c.2374C > T (p.Arg792*)), 1 in-frame deletion (c.2137_2145del (p.Gln713_Leu715del)), 1 splice site mutation (c.3718-12A > G (IVS27-12A > G)), and 1 missense mutation (c.1556C > T (p.Thr519Met)). Based on patient phenotypes and previous functional studies, these variants could be classified as complete loss-of-function, partial loss-of-function, or gain-of-function. Complete loss-of-function variants include NMD-elicit variants

c.208del (p.Asp70Ilefs*18), c.1263_1264delAA (p.Gln421Hisfs*11), c.2374C > T (p.Arg792*), c.3394_3403del (p.Gln1132Serfs*30) and in-frame deletion c.2137_2145del (p.Gln713_Leu715del). NMD promotes the degradation of mutant transcripts containing PTCs, resulting in decreased absolute expression levels. While NMD efficiency may not always reach 100 % [17], some truncated proteins lacking at least the carboxy-terminal KIM, $p75^{NTR}$ and PDZ-binding regions are produced. A previous study revealed that the KIM region binds to KLC1 and KLC2 to regulate the intracellular trafficking processes of the *KIDINS220* and receptor complexes by recruiting the kinesin-1 motor complex [31]. PC12 cells lacking the functional KIM region of *KIDINS220* exhibits impaired axonal transport, defects in neurotrophin signaling, and neurite differentiation [31]. In addition, *KIDINS220* binds to TrkA and mediates TrkA phosphorylation signaling, activating the PI3Kinase-AKT and Ras-MAPK pathways, which regulate neuronal survival, neurite growth, and differentiation. The binding between c.2137_2145del (p.Gln713_Leu715del) and TrkA is impaired, resulting in the complete loss of *KIDINS220* function [19]. Compared with complete loss-of-function variants, AR-SINO related splice site variants c.3718-12A > G (IVS27-12A > G) and missense variants c.1556C > T (p.Thr519Met) retain a certain level of normal transcripts or functional domains, representing partial loss-of-function. Zhang et al. demonstrated that the pathogenic nonsense variant c.4177C > T (p.Q1393*) escapes NMD and produces gain-of-function truncated protein with weak affinity for calpain-2 [14]. Due to the blockage of degradation, the accumulation of gain-of-function truncated protein leads to hyperactivation of Rac1 and defects in neuronal development [14]. Considering the distribution of pathogenic and non-pathogenic NMD-escape variants [9,16,17], we further propose that the deletion of amino acid residues 1507–1529 at the potential recognition site of calpain-2, especially K1508 and P1520, may determine the functional acquisition characteristics of the variants and the phenotypes of AD-SINO. We can draw insights from these results. Biallelic loss-of-function variants in *KIDINS220* underlie VENARG and AR-SINO. The former is caused by two copies of complete loss-of-function, while the latter is caused by one copy of complete loss-of-function and one copy of partial loss-of-function. The heterozygous gain-of-function variant involving the deletion of amino acid residues 1507–1529, especially K1508 and P1520, underlies AD-SINO. However, determining the function of mutations remains a challenging issue. Although several predictive tools are available, investigating phenotype-genotype correlations for rare cases is a prerequisite.

In summary, the compound heterozygous variants identified in this study are novel and suggest an autosomal recessive inheritance pattern for SINO syndrome in this family. This study expands the spectrum of *KIDINS220* gene etiological variants, phenotypes, and genetic patterns associated with SINO syndrome. Moreover, it provides insights into potential genotype-phenotype correlations based on known *KIDINS220* variants and related clinical features. These insights may aid in understanding pathogenic mechanisms, developing gene therapeutic strategies for SINO or VENARG, and guiding future pregnancies to reduce the risk of recurrence.

Data Availability statement

Data included in article/supplementary material/referenced in article.

Ethics statement

The study was approved by the Ethics Committee of Henan Provincial People's Hospital (approval number: 2019_134) and all subjects signed informed consent. The study adhered to the tenants of Declaration of Helsinki.

Funding

This work was supported by the Major and Key Projects Jointly Constructed by Henan Province and Ministry of Science and Technology (Grant No. SBGJ202101003 and SBGJ202302014), and Scientific Research Startup Funds of Henan Provincial People's Hospital (Grant No. ZC20190149 and ZC20220268).

CRediT authorship contribution statement

Wenke Yang: Writing – original draft, Visualization, Methodology, Investigation, Funding acquisition, Conceptualization. **Shuyue Wang:** Writing – original draft, Visualization, Methodology, Investigation, Conceptualization. **Xiaodong Huo:** Visualization, Methodology, Investigation. **Ke Yang:** Visualization, Methodology. **Zhenglong Guo:** Project administration, Conceptualization. **Yanjun Li:** Visualization, Validation. **Xinying Ji:** Writing – review & editing, Supervision, Formal analysis, Conceptualization. **Bingtao Hao:** Writing – review & editing. **Shixiu Liao:** Writing – review & editing, Supervision, Methodology, Funding acquisition, Conceptualization.

Declaration of competing interest

The authors declare that they have no competing interests to declare.

Acknowledgments

The authors would like to thank all participants for their assistance and cooperation in this study.

Appendix A. Supplementary data

Supplementary data to this article can be found online at https://doi.org/10.1016/j.heliyon.2024.e37355.

References

[1] T. Iglesias, N. Cabrera-Poch, M.P. Mitchell, et al., Identification and cloning of Kidins220, a novel neuronal substrate of protein kinase D, J. Biol. Chem. 275 (51) (2000) 40048–40056.
[2] H. Kong, J. Boulter, J.L. Weber, et al., An evolutionarily conserved transmembrane protein that is a novel downstream target of neurotrophin and ephrin receptors, J. Neurosci. 21 (1) (2001) 176–185.
[3] M.S. Chang, J.C. Arevalo, M.V. Chao, Ternary complex with Trk, p75, and an ankyrin-rich membrane spanning protein, J. Neurosci. Res. 78 (2) (2004) 186–192.
[4] F. Cesca, A. Yabe, B. Spencer-Dene, et al., Kidins220/ARMS mediates the integration of the neurotrophin and VEGF pathways in the vascular and nervous systems, Cell Death Differ. 19 (2) (2012) 194–208.
[5] J. Scholz-Starke, F. Cesca, G. Schiavo, et al., Kidins220/ARMS is a novel modulator of short-term synaptic plasticity in hippocampal GABAergic neurons, PLoS One 7 (4) (2012) e35785.
[6] V.E. Neubrand, F. Cesca, F. Benfenati, et al., Kidins220/ARMS as a functional mediator of multiple receptor signalling pathways, J. Cell Sci. 125 (Pt 8) (2012) 1845–1854.
[7] Y. Chen, W.Y. Fu, J.P. Ip, et al., Ankyrin repeat-rich membrane spanning protein (kidins220) is required for neurotrophin and ephrin receptor-dependent dendrite development, J. Neurosci. 32 (24) (2012) 8263–8269.
[8] N. Schmieg, C. Thomas, A. Yabe, et al., Novel Kidins220/ARMS splice isoforms: potential specific regulators of neuronal and cardiovascular development, PLoS One 10 (6) (2015) e0129944.
[9] D.J. Josifova, G.R. Monroe, F. Tessadori, et al., Heterozygous KIDINS220/ARMS nonsense variants cause spastic paraplegia, intellectual disability, nystagmus, and obesity, Hum. Mol. Genet. 25 (11) (2016) 2158–2167.
[10] L. Yang, W. Zhang, J. Peng, et al., Heterozygous KIDINS220 mutation leads to spastic paraplegia and obesity in an Asian girl, Eur. J. Neurol. 25 (5) (2018) e53–e54.
[11] M. Zhao, Y.J. Chen, M.W. Wang, et al., Genetic and clinical profile of Chinese patients with autosomal dominant spastic paraplegia, Mol. Diagn. Ther. 23 (6) (2019) 781–789.
[12] K. Zhang, W. Sun, Y. Liu, et al., SINO syndrome causative KIDINS220/ARMS gene regulates adipocyte differentiation, Front. Cell Dev. Biol. 9 (2021) 619475.
[13] Angela Lee, Luque Jorge Granadillo De, P225: SINO syndrome associated with heterozygous KIDINS220 variants: a more severe presentation and maternal mosaicism, Genetics in Medicine Open 1 (1) (2023) 100253, https://doi.org/10.1016/j.gimo.2023.100253. Supplement.
[14] J. Zhang, Y. Zhang, Q. Shang, et al., Gain-of-Function KIDINS220 variants disrupt neuronal development and cause cerebral palsy, Mov. Disord. 39 (3) (2024) 498–509.
[15] I.L. Mero, H.H. Mørk, Y. Sheng, et al., Homozygous KIDINS220 loss-of-function variants in fetuses with cerebral ventriculomegaly and limb contractures, Hum. Mol. Genet. 26 (19) (2017) 3792–3796.
[16] R.G.H. Lindeboom, M. Vermeulen, B. Lehner, et al., The impact of nonsense-mediated mRNA decay on genetic disease, gene editing and cancer immunotherapy, Nat. Genet. 51 (11) (2019) 1645–1651.
[17] R.G. Lindeboom, F. Supek, B. Lehner, The rules and impact of nonsense-mediated mRNA decay in human cancers, Nat. Genet. 48 (10) (2016) 1112–1118.
[18] S.H. El-Dessouky, M.Y. Issa, M.M. Aboulghar, et al., Prenatal delineation of a distinct lethal fetal syndrome caused by a homozygous truncating KIDINS220 variant, Am. J. Med. Genet. 182 (12) (2020) 2867–2876.
[19] V. Jacquemin, M. Antoine, S. Duerinckx, et al., TrkA mediates effect of novel KIDINS220 mutation in human brain ventriculomegaly, Hum. Mol. Genet. 29 (23) (2021) 3757–3764.
[20] L.I. Brady, B. DeFrance, M. Tarnopolsky, Pre- and postnatal characterization of autosomal recessive kidins220-associated ventriculomegaly, Mol. Syndromol. 13 (5) (2022) 419–424.
[21] Z. Guo, B. Kang, D. Wu, et al., Case report: twin pregnancy gives birth to a girl with partial trisomy 21 mosaicism after in vitro fertilization and embryo transfer, Front. Genet. 12 (2021) 740415.
[22] X. Hai, G. Liangjie, Z. Qian, et al., Genetic analysis of a case of sotos syndrome with suspected germinal mosaicism in mother, Appl. Biochem. Biotechnol. 195 (10) (2023) 5792–5801.
[23] H. Li, R. Durbin, Fast and accurate short read alignment with Burrows-Wheeler transform, Bioinformatics 25 (14) (2009) 1754–1760.
[24] A. McKenna, M. Hanna, E. Banks, et al., The Genome Analysis Toolkit: a MapReduce framework for analyzing next-generation DNA sequencing data, Genome Res. 20 (9) (2010) 1297–1303.
[25] K. Wang, M. Li, H. Hakonarson, ANNOVAR: functional annotation of genetic variants from high-throughput sequencing data, Nucleic Acids Res. 38 (16) (2010) e164.
[26] S. Richards, N. Aziz, S. Bale, et al., Standards and guidelines for the interpretation of sequence variants: a joint consensus recommendation of the American College of medical genetics and genomics and the association for molecular pathology, Genet. Med. 17 (5) (2015) 405–424.
[27] A. Hamosh, A.F. Scott, J.S. Amberger, et al., Online Mendelian Inheritance in Man (OMIM), a knowledgebase of human genes and genetic disorders, Nucleic Acids Res. 33 (Database issue) (2005) D514–D517.
[28] M.J. Landrum, J.M. Lee, M. Benson, et al., ClinVar: public archive of interpretations of clinically relevant variants, Nucleic Acids Res. 44 (D1) (2016) D862–D868.
[29] P.D. Stenson, M. Mort, E.V. Ball, et al., The Human Gene Mutation Database: towards a comprehensive repository of inherited mutation data for medical research, genetic diagnosis and next-generation sequencing studies, Hum. Genet. 136 (6) (2017) 665–677.
[30] A. Almacellas-Barbanoj, M. Albini, A. Satapathy, et al., Kidins220/ARMS modulates brain morphology and anxiety-like traits in adult mice, Cell Death Discov 8 (1) (2022) 58.
[31] A. Bracale, F. Cesca, V.E. Neubrand, et al., Kidins220/ARMS is transported by a kinesin-1-based mechanism likely to be involved in neuronal differentiation, Mol. Biol. Cell 18 (1) (2007) 142–152.
[32] A. Del Puerto, J. Pose-Utrilla, A. Simón-García, et al., Kidins220 deficiency causes ventriculomegaly via SNX27-retromer-dependent AQP4 degradation, Mol Psychiatry 26 (11) (2021) 6411–6426.
[33] F. Cesca, A. Satapathy, E. Ferrea, et al., Functional interaction between the scaffold protein Kidins220/ARMS and neuronal voltage-gated Na+ channels, J. Biol. Chem. 290 (29) (2015) 18045–18055.